Experimental study of an externally finned tube with internal heat transfer enhancement for phase change thermal energy storage

M Martinelli [1,2,a], F Bentivoglio [1], R Couturier [1], J-F Fourmigué [1], P Marty [2]

[1] LITEN, CEA Grenoble, 17 rue des Martyrs, 38054 Grenoble Cedex 9, France
[2] LEGI, Université Grenoble Alpes, BP 53, 38041 Grenoble Cedex 9, France

matthieu.martinelli@cea.fr

Abstract. After having presented the design of a latent heat thermal energy storage system (LHTESS) for district heating, experimental results of a vertical tube-in-shell LHTESS are discussed. The tube is radially finned on its external wall to enhance the heat transfer in the phase change material. The test rig is operated with flow conditions corresponding to the proposed design. As the internal flow of heat transfer fluid (HTF) appears to be laminar and is highly influenced by buoyancy forces, which results in mixed convection regime, cross-sectional area reducers are installed inside the HTF tube in order to reduce the Rayleigh number and thus natural convection. Experimental results are presented for two finned tubes, with and without internal heat transfer enhancement respectively.

1. Introduction

Evening the discrepancies between energy offer and supply is a key point of effectiveness for many applications such as district heating network (DHN). In the framework of DHN, thermal energy storage (TES) is a proven efficient way to smooth these discrepancies out. Besides, TES appears to be an attractive option for effectiveness since it adds flexibility, helps to reduce CO_2 emissions and is cost-effective [1]. In particular, latent heat thermal energy storage systems (LHTESS) are a promising way to store thermal energy. As a matter of fact, using a phase change material (PCM) is quite attractive due to potential high storage density and constant temperature heat source.

Several heat exchanger technologies are investigated for LHTESS. Among them, the shell-and-tube one accounts for more than 70% of previously published papers dealing with LHTESS [2]. Given that the majority of non-metallic PCM with high phase change enthalpy have one major drawback which is a poor thermal conductivity (<1 W/m/K) [3], the main thermal resistance is usually on the PCM side. As a result, a lot of studies focus on heat transfer enhancement techniques on the PCM side. The most common solution consists in adding fins around the tubes [2]. As soon as 1981, De Jong and Hoogendoorn [4] compared experimentally a simple tube with two differently finned tubes and concluded that solidification rate was 27 times faster with fins than without. Erek et al. [5] conducted an experimental comparison on 7 tubes, including 6 finned tubes. One of the main results of the study is that the heat transfer from the HTF (Heat Transfer Fluid) to the PCM increased with increasing fin diameter and fins density. Sasaguchi et al. [6], who studied longitudinally and radially finned tubes, stressed the fact that heat transfer exchange area is of prime importance in order to increase the thermal

[a] To whom any correspondence should be addressed.

Keywords: Thermal energy storage; Phase change material; District heating; Finned tube; Internal insert

performances for both the solidification and the melting processes. It is worth noting that among the considerable number of studies concerning shell-and-tube LHTESS, two main trends are followed: either the HTF mass flow rate is high, the flow is turbulent, and the temperature difference between the inlet and the outlet is small, even negligible (thus obtaining a constant wall temperature), or the HTF mass flow rate is small, the flow is laminar and the temperature difference between the inlet and the outlet is significant. The latest is more representative of an industrial system such as DHN where the purpose is to heat the fluid up.

Increasing the effective thermal conductivity on the PCM side is relevant since the PCM thermal conductivity generally is low. Nevertheless, a low-Reynolds-number internal flow and a low-Prandtl-number fluid may result in a low convective heat transfer coefficient between the HTF and the tubes. Besides, if the tubes are externally finned, the main thermal resistance may occur to be on the HTF side rather than on the PCM side. Moreover, a low-Reynolds-number flow combined with a high Rayleigh number can result in mixed convection which can increase (aided mixed convection) or decrease (opposed mixed convection) the heat transfer coefficient [7]. Above a certain threshold of buoyancy force, the flow will become unstable and modify the expected thermal behaviour of the test rig. It will be shown that these conditions can easily be gathered for LHTESS installed in a DHN. Colella et al. [8] are the first known to have designed and numerically analysed a LHTESS for a DHN. In doing so, they attested the interest of LHTESS on DHN. Concerning the HTF flow conditions, they found a Reynolds number ranging from 500 to 2000. Taking a closer look to the operating conditions they chose, it appears that the Rayleigh number is high ($Ra = 4.6\ 10^7$) and that the flow regime is not laminar as expected and considered in the study, but characteristic of a "turbulent flow of mixed convection" [9].

In this study, a tube-in-shell test rig is set up on a hydraulic loop and operated in near real DHN operating conditions. Heat transfer enhancement systems are investigated both inside the HTF and on the PCM side. As a matter of fact, two different externally radially finned tubes are tested, with 7 fpi (*fins per inch*) and 10 fpi respectively. The fins extend up to the shell inner surface. Thermal performance for both tubes are studied with and without tube cross-sectional area reducers, namely an insert. The aim of the study is to assess the recourse to internal insert in order to eliminate the possibility to get an unstable HTF flow.

2. Flow regime inside a standard LHTESS for DHN

2.1. Standard sizing of a LHTESS for DHN

Let H and D be the height and the diameter of a shell-and-tube LHTESS with a cylindrical tank. HTF power and mass flow rate, as well as PCM latent heat content and mass, can be expressed as:

$$P = \dot{m}\, c_{p,htf} \left(T_{htf}^{out} - T_{htf}^{in}\right) = \frac{\mathrm{E_{pcm}}}{\Delta \mathrm{t}} \tag{1}$$

$$\dot{m} = \bar{V}\, \rho_{htf} \times \frac{\pi\, d^2}{4} \times N \tag{2}$$

$$E_{pcm} = m_{pcm}\, \Lambda \tag{3}$$

$$m_{pcm} = \frac{\pi D^2}{4} H\, \rho_{pcm} \times \epsilon \tag{4}$$

where Δt is the theoretical time for the LHTESS to store/release the latent heat content E with a constant power P; $\bar{V}$ is the cross-sectional averaged HTF velocity; N the number of tubes inside the tank; m_{pcm} the mass of PCM inside the tank and ϵ the volumetric fraction of PCM inside the tank (remaining space being occupied by the tubes and the fins). Let χ be the fraction of fin diameter on tube inner diameter:

$$\chi = \frac{d_{fin}}{d} \tag{5}$$

In a cylindrical tank, radially finned tube with circular fins do not occupy the whole cross-sectional area. As a matter of fact, it can be considered that the used cross-sectional area, for each tube, is in the shape of a hexagon. Which means that the cross-sectional area used by the tubes is approximately $\xi =$

91%, that is area of the inscribed circle of the hexagon, divided by the actual area of the hexagon. As a result, N can be expressed as:

$$N = \frac{D^2}{d^2 \chi^2 \xi} \tag{6}$$

Combining all the precedent expressions it can be stated that:

$$Re = 4\frac{\dot{m}}{\pi\, d\, \mu} = \frac{\chi^2 \epsilon\, \Lambda\, \rho_{pcm}}{\xi \left(\mu\, c_p\, (T^{out} - T^{in})\right)_{htf}} \times \frac{H}{\Delta t} \times d \tag{7}$$

The final sizing is given in the Table 1. Obviously, all the presented parameters are variable and the Reynolds number value is not fixed and constant for all LHTESS on DHN. However, it should be noted that a real sizing is currently undertaken for the DHN Company of Grenoble (France) and that the proposed values are similar to those selected in the real design.

Table 1. Common values from the existing state of the art for finned-tube-in-shell LHTESS [1;3-6;8;10-12] is on the first line and selected parameters are on the second

ϵ [-]	χ [-]	d [mm]	$\rho_{pcm}\Lambda$ [MJ/m^3]	Δt [hrs]	ΔT_{in}^{out} [°C]	H [m]
[0.8,0.9]	[2,5]	[10,37]	[200,300]	[1,2]	[20,40]	{2.9}
80%	3.0	20	250	2	20	3

2.2. Flow characterisation

With water (Table 2) as HTF, the Reynolds number equals approximately 325. Using few tubes with a smaller inner diameter and wider fins and opt for a higher tank will results in higher Reynolds number. Nevertheless, as a consequence the mass flow rate will be higher and heating the HTF up will be more complicated since the temperature difference between the inlet and the outlet will drop [8]. As it was showed by Colella et al. [8], it is highly recommended to choose a small mass flow rate per tube.

Table 2. Properties of water at 70°C [13].

Material	ρ [kg/m^3]	c_p [J/kg/K]	μ [kg/s/m]	β [1/K]	λ [W/m/K]
water	978	4190	4.04 10^{-4}	5.84 10^{-4}	0.663

Keeping the same conditions, the Rayleigh number is equal to 2.05 10^7, with the tube diameter as the characteristic length and assuming that the HTF outlet temperature is near the phase change temperature, the temperature difference is 30°C. Looking at the Metais and Eckert's [9] diagram (Figure 1), the resulting flow regime appears to be under laminar-turbulent transitional conditions, with mixed convective heat transfer mode.

Since LHTESS are neither under uniform wall temperature nor uniform heat flux condition, besides the functioning is not stationary, thus the theoretical heat transfer coefficient is hard to predict.

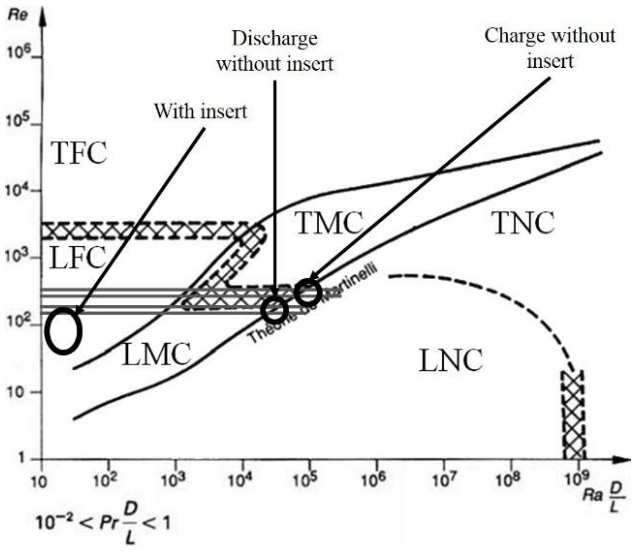

Figure 1. Regimes of natural (N), forced (F) and mixed (M) convection (C) for flow through vertical tubes [9]. 'L' and 'T' are for 'laminar' and 'turbulent' respectively.

3. Material and Method

Experimental set up consists in a hydraulic loop with two water baths, two pumps and the test rig where the heat exchanger is located. One bath is used as a cooler (~20 °C) meanwhile the second is used as a heater (~50 °C). Both cold and hot flows run in parallel, while one flows through the test rig, the second is bypassed. Consequently, it is possible to alternate melting and solidification. Furthermore, the experimental set up enables upward and downward flows. HTF temperature is measured at the inlet and at the outlet of the test rig, thanks to a thermocouple situated on the symmetry axis.

The phase change material (PCM) is a paraffin (RT35HC from Rubitherm®) and is located on the shell side while water is used as the heat transfer fluid (HTF) and is circulated throughout the central tube. Data for the used PCM are summed up in the Table 3, phase change enthalpy is measured thanks to a Setaram®-C80 calorimeter (20 to 50 °C, at 0.05 °C/min) on a temperature range of 5 °C. The shell inner and outer diameters are 61 and 70 mm respectively. The tube inner and outer diameters are approximately $18.5^{(+/-0.5)}$ and 25.4 mm respectively. The fins are 57.5 mm in diameter, 0.35 mm in thickness and fins density is 7 and 10 fpi respectively for the two test rigs (that is 3.3 and 2.2 mm in pitch respectively) (Figure 3). The test rig is 400 mm long and is placed vertically. Mass flow rate is measured with a MicroMotion® Coriolis flowmeter and is fixed to 9 kg/h. HTF inlet temperature is 20 or 50 °C for discharging and charging process respectively. Initially, the test rig is maintained at 20 or 50 °C depending on the process. Consequently, Stefan number equals 0.13 and 0.14 for charging and discharging process respectively. 40 calibrated K-type thermocouples are regularly installed in the PCM and enable the recording of the temperature.

Table 3. RT35HC PCM properties. Bold characters are for measured properties.

Material	ρ_{liq} [kg/m^3]	ρ_{sol} [kg/m^3]	Λ [J/g]	$T_{\text{phase change}}$ [°C]
RT35HC	770	880	**230**	35

Tests are carried out without and with internal insert (Figure 2). The internal insert is a plastic cylinder equipped with short plastic rods for the cylinder to be centred inside the HTF tube. Inserts are designed such as the annular duct is 1 mm wide. As a result, the hydraulic diameter is ten times smaller than without insert. It is worth noting that in the Metais and Eckert's [9] diagram (Figure 1), natural convection is a function of the characteristic length at the power of 4. Consequently, the buoyancy forces influence is divided by 10^4 with the insert. In doing so, the Reynolds number will drop too and the resulting flow regime is a laminar flow with mainly laminar forced convection.

Figure 2. Cylindrical insert used as cross-sectional area reducer.

Figure 3. Sample of the tested finned tube. The fins density is 10 fpi here.

Operating conditions are represented on the Figure 1, HTF properties are calculated at the inlet temperature [13]. Experimental operating conditions are represented with circles. The lines represent the possible values throughout the experiment. Dimensionless numbers are calculated for temperature differences ranging from 30 to 0°C to cover the whole process from the start ($\Delta T_{pcm}^{htf} = 30$ °C) to the end ($\Delta T_{pcm}^{htf} = 0$ °C). It appears clearly that internal inserts reduce considerably the Rayleigh number and thus natural convection heat transfer. The Nusselt-Graetz solution for the calculation of the mean convective heat transfer coefficient for thermally developing and hydrodynamically developed laminar flow in contact with an isothermal wall gives approximately 180 W/m^2/K without insert and 7.6 times more with insert [7]. The overall convective heat transfer coefficient increases with decreasing hydraulic diameter.

Thanks to the 40 thermocouples distributed regularly throughout the test rig, the progression of the phase change front inside the test rig is tracked. An experimental method, based on the calculation of the energy stored by the PCM enables to define a characteristic fusion/solidification time. It is assumed that the 40 thermocouples represent a mesh and that for each thermocouple corresponds a given quantity of PCM. This method is similar to the one presented by Caron et al. [14].

For each presented configuration, a minimum of 3 tests are carried out in order to assess the repeatability.

4. Results and discussion

4.1. Without internal insert

Figure 4 shows HTF inlet and outlet temperature during discharge with bottom injection (aided mixed convection). It is worth noting that the representative curve for inlet temperature is smooth, whereas the one for the outlet temperature is noisy. Buoyancy forces compete with inertial forces, resulting in a recirculation loop inside the HTF tube and causing the noise to appear on the recording.

Concerning top injection, Figure 5 shows outlet temperature for 3 tests with an inlet temperature of 20 °C. The outlet temperature representative curves are not noisy unlike the bottom injection case (Figure 4).

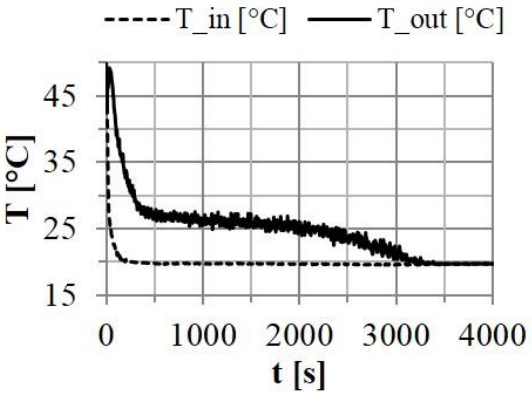

Figure 4. HTF inlet and outlet temperatures during a discharge with bottom injection (HTF with upward flow) with the 10 fpi tube.

Figure 6 presents 4 tests with inlet temperature at 15 °C. To start with, only the 3 tests with a noisy outlet temperature representative curve are considered. Firstly, it appears that lowering the inlet temperature from 20 to 15 °C reduces the inlet-outlet temperature difference, which means a reduced power and thus an increase in the necessary time to complete the phase change. This result is counter-intuitive, since reducing the HTF inlet temperature increases the Stefan number and should accelerate the phase change. Secondly, the noisy curves indicates that flow regimes are different between the 20 °C injection temperature case and the 15 °C injection one.

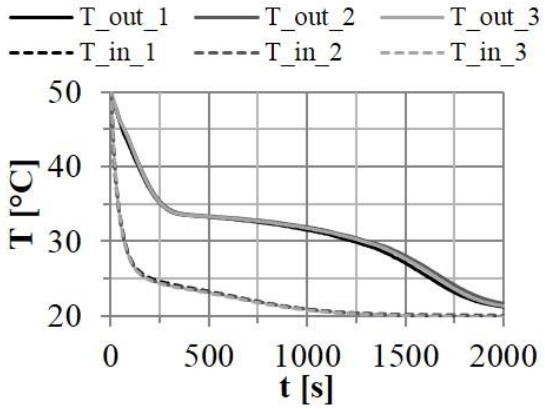

Figure 5. HTF outlet temperature during a discharge with top injection (HTF with downward flow) at 20 °C with the 10 fpi tube.

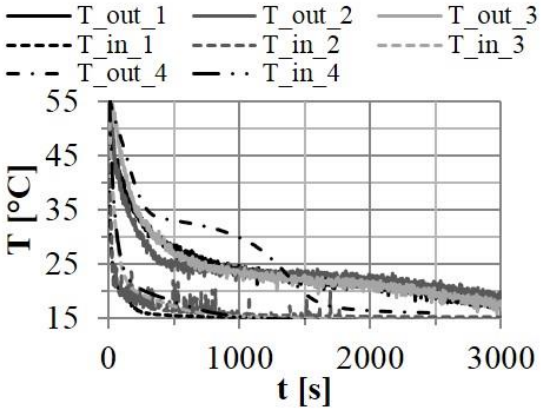

Figure 6. HTF outlet temperature during a discharge with top injection (HTF with downward flow) at 15 °C with the 10 fpi tube.

The 4th test with a HTF inlet temperature of 15 °C (Figure 6) is carried out with a mass flow rate of 9.3 kg/h, meaning a +3% in comparison with other tests that are carried out at 9 kg/h. It is clear that the

outlet temperature curve is not noisy and that the transferred power is higher since inlet-outlet temperatures difference is high. It can then be concluded that the flow regime is highly instable and can easily switch from one flow regime configuration to another (Figure 1).

Flow regime is heavily influenced by PCM temperature as well as HTF inlet temperature. Indeed, Figure 7 shows that HTF inlet temperature curve is initially noisy and becomes smooth after 2 750 s. One should note that inlet temperature is 20 °C but the inlet thermocouple records temperatures ranging from 20 to 25 °C, meaning that hot water are recirculating in the pipe. It is worth noting that 25 °C is close to the outlet temperature. By looking at Figure 8 it is clear that 2 750 s corresponds to the moment when the PCM is solid everywhere, meaning the undercooling is beginning and the temperature difference between the tube wall and the HTF is decreasing. Thus the Rayleigh number decreases as well, which enables to switch from one flow regime to another.

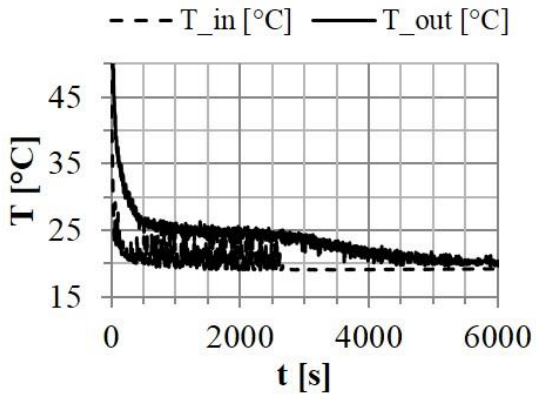

Figure 7. HTF inlet and outlet temperatures during a discharge with top injection at 20 °C with the 7 fpi tube.

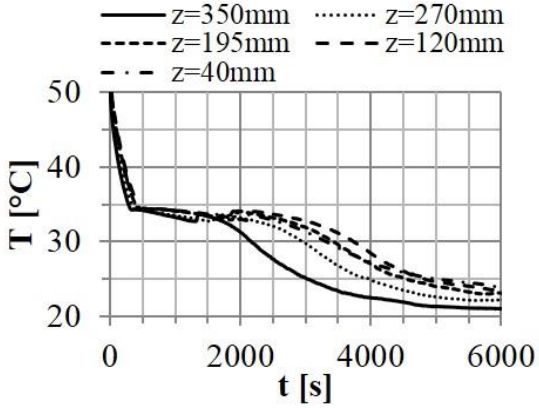

Figure 8. PCM temperatures during a discharge with top injection at 20 °C with the 7 fpi tube. Thermocouples are at a radial distance of 19 mm.

4.2. With internal insert

Looking at the Table 4, one can note that internal inserts show good performance and provide more homogeneous results between charge and discharge and between downward and upward flows. It appears that the thermal behaviour of the PCM is essentially conducted by conduction heat transfer since phase change time is independent of the HTF flow direction and the process. Besides, it indicates that the differences among the results obtained without internal insert are mainly explained by HTF flow regime rather than by the fins or the operating conditions (downward/upward). Moreover, it can be seen that 10 fpi tubes have characteristic times $12^{(+/-2)}$ % lower than 7 fpi tubes.

Without insert, performances appears to be highly unpredictable. The most meaningful one, is the characteristic time difference for the discharging process with downward flow between the 7 and the 10 fpi tubes: 3 240 and 1 490 s respectively. Such a difference cannot be explain by the change in fins density as it accounts for less than 15%. The main difference is thus in the HTF flow regime (Rayleigh numbers are slightly different) and is visible on the HTF temperature representative curves since they are noisy for the 7 fpi tube (Figure 7) and smooth for the 10 fpi tube (Figure 5).

It is worth noting that the heat transfer coefficient is not always better with the internal inserts as it would be expected if the buoyancy forces weren't taken into account. Indeed, the characteristic times for melting with downward flow are always lower without insert rather than with. Whereas it has been calculated that the convective heat transfer coefficient for laminar forced flow is 7.6 times higher with insert rather than without. Actually, charge with downward flow is representative of aided mixed convection: heat transfer performances are better than for a forced laminar flow case thanks to buoyancy forces.

Taking a closer look at the discharge with downward flow cases, it appears that the solidification for the 7 fpi tube is faster with insert, whereas the solidification for the 10 fpi tube is faster without insert. Considering the no-insert case, the opposed mixed convection should lower the convective heat transfer coefficient in comparison with the laminar-forced-flow case. Concerning the case with insert, the laminar-forced-flow convective heat transfer coefficient should be higher than for the no-insert case. All together the heat transfer performances are supposed to be better with the insert. Nevertheless, as said before, buoyancy forces can lead to unstable flow that can locally increase the heat transfer coefficient. Actually, it has been shown that, for a Grashof number of $3x10^6$ (experimental values are between 1 and $3x10^6$), the overall heat transfer for low-Reynolds-flow with mixed convection under transitional conditions in a pipe with uniform wall temperature is higher for the opposed case than for the aided case [7]. Which means that instabilities actually increase the overall heat transfer. Despite, it must be stressed that the representative curve for the HTF temperature are smooth (Figure 5), meaning that there is no recirculation loop.

Finally, in the framework of DHN, discharge is the critical process since fast response time and high power are requested and upward flow is the most expected configuration. With the tested configurations and conditions, discharges with upward flow are always carried out faster with internal inserts.

Table 4. Averaged characteristic times for charging/discharging, with and without insert, for the 7 and 10 fpi tubes. For each configuration, the presented value is the average for 3 repeatable tests.

$t_{characteristic}$ [s]		7 fpi		10 fpi	
		Without insert	With insert	Without insert	With insert
Charge	Downward flow	1840	1860	1310	1600
	Upward flow	2650	1780	2640	1530
Discharge	Downward flow	3240	1950	1490	1730
	Upward flow	2810	1840	2620	1710

5. Conclusion

In conclusion, under operating conditions such as those which can be encountered when integrating a LHTESS on a DHN, the internal flow of the HTF can be influenced by buoyancy forces. It has been shown that, without internal inserts, flow regime can easily become unstable, is highly unpredictable and sometimes unreproducible. Such conditions are not favourable to operate an installation.

By adding internal insert, the Rayleigh number is divided by 10^3 and the flow regime switch from an unstable flow (mixed convection under transitional flow) to a laminar flow with forced convection mainly. With internal inserts, the flow regime is modified, which provides repeatability, better regularity for the phase change front progression and more reliable heat transfer performances. Furthermore, reducing the hydraulic diameter increases the laminar-flow-forced-convection heat transfer coefficient, as well as increasing the fins density.

It is highly recommended, when designing a LHTESS for DHN to look at the Rayleigh number and to estimate the buoyancy forces influence on the flow regime. So, it may be necessary to implement internal inserts in order to modify the flow regime and get more reliable operating conditions.

6. Acknowledgement

The authors gratefully acknowledge the financial support from the Grenoble (France) district heating company (CCIAG).

7. Nomenclature

c_p	Specific heat capacity [J/g/K]
d	Tube inner diameter [m]
D	Tank diameter [m]
E	Latent heat content [J/g]
g	Gravity of Earth [m^2/s]
h	Heat transfer coefficient [W/m^2/K]
H	Tank height [m]
$m/\dot{m}$	Mass [g] / Mass flow rate [g/s]
N	Number of tubes in the tank
P	Power [W]
Δt	Time to store/release energy [s]
T	Temperature [°C or K]
$\bar{V}$	Mean velocity [m/s]
z	Height [m]
Greek symbols	
α	Thermal diffusivity [m^2/s]
β	Thermal expansion [1/K]
ϵ	Effective porosity [-]
λ	Thermal conductivity [W/m/s]
Λ	Phase change enthalpy [J/g]
μ	Dynamic viscosity [g/m/s]
ν	Kinematic viscosity [m^2/s]
ξ	Fraction of the cross-sectional area of the tank actually occupied by the finned tubes [-]
ρ	Density [g/m^3]
χ	Fraction of fin diameter on tube inner diameter [-]

Subscripts & superscripts	
htf	Heat Transfer Fluid
in	inlet
liq	liquid
pcm	Phase Change Material
out	outlet
sol	solid
Dimensionless numbers	
Gr	$= \frac{g\beta\lvert T_{in}^{htf} - T_{wall}\rvert d^3\rho^2}{\mu^2}$
Re	$= \frac{\rho\bar{V}d}{\mu}$
Ra	$= \frac{g\beta\lvert T_{in}^{htf} - T_{wall}\rvert d^3}{\nu\alpha}$
Ste	$= \frac{c_p\lvert T_{phase\ change} - T_{in}^{htf}\rvert}{\Lambda}$

References

[1] Gadd H and Werner S 2015 *Advances in Thermal Energy Storage Systems: Methods and Applications - Thermal energy storage systems for district heating and cooling* Ed L F Cabeza (Cambridge: Woodhead Publishing Series in Energy) 66 pp 467-78.
[2] Agyenim F, Hewitt N, Eames P and Smyth M 2010 *Renewable and Sustainable Energy Reviews* **14** pp 615-628
[3] Mehling H and Cabeza L F 2008 - *Heat and cold storage with PCM* Eds D Mewes and F Mayinger Springer).
[4] De Jong A G and Hoogendoorn C J 1981 *Thermal Storage of Solar Energy - Latent Heat Storage* Ed C den Ouden (The Hague: Martinus Nijhoff Publishers) pp 123-33.
[5] Erek A, Ilken Z and Acar M A 2005 *Int. J. Energy Res.* **29** pp 283-301
[6] Sasaguchi K, Yoshida M and Nakashima S 1990 *Heat Transfer - Japanese Research* **19** pp 11-27
[7] 2008 *Heat Exchanger Design Handbook - Part 2: Fluid Mechanics and Heat Transfer* Ed G F Hewitt (Connecticut: Begell House Publishers, Inc.).
[8] Colella F, Sciacovelli A and Verda V 2012 *Energy* **45** pp 397-406
[9] Metais B and Eckert E R G 1964 *Journal of Heat Transfer* **86** pp 295-296
[10] Merlin K, Delaunay D, Soto J and Traonvouez L 2016 *Applied Energy* **166** pp 107-116
[11] Medrano M, Yilmaz M O, Nogués M, Martorell I, Roca J and Cabeza L F 2009 *Applied Energy* **86** pp 2047-2055
[12] Lacroix M 1993 *International Journal of Heat and Mass Transfer* **36** pp 2083-2092
[13] 2016 *NIST Chemistry WebBook, NIST Standard Reference Database Number 69* Eds P J Linstrom and W G Mallard (Gaithersburg: National Institute of Standards and Technology).
[14] Caron-Soupart A, Fourmigué J F, Marty P and Couturier R 2016 *Applied Thermal Engineering* **98** pp 1286-1296